Journal of Microbiology (2022) Vol. 60, No. 8, pp. 859–866
DOI 10.1007/s12275-022-2107-y
eISSN 1976-3794
pISSN 1225-8873

Eradication of drug-resistant *Acinetobacter baumannii* by cell-penetrating peptide fused endolysin[§]

Jeonghyun Lim[1], Jaeyeon Jang[1], Heejoon Myung[1,2], and Miryoung Song[1*]

[1]*Department of Bioscience and Biotechnology, Hankuk University of Foreign Studies, Yongin 17035, Republic of Korea*
[2]*LyseNTech Co., Ltd., Seongnam 13486, Republic of Korea*

(Received Mar 7, 2022 / Revised May 3, 2022 / Accepted May 4, 2022)

Antimicrobial agents targeting peptidoglycan have shown successful results in eliminating bacteria with high selective toxicity. Bacteriophage encoded endolysin as an alternative antibiotics is a peptidoglycan degrading enzyme with a low rate of resistance. Here, the engineered endolysin was developed to defeat multiple drug-resistant (MDR) *Acinetobacter baumannii*. First, putative endolysin PA90 was predicted by genome analysis of isolated *Pseudomonas* phage PBPA. The His-tagged PA90 was purified from BL21(DE3) pLysS and tested for the enzymatic activity using Gram-negative pathogens known for having a high antibiotic resistance rate including *A. baumannii*. Since the measured activity of PA90 was low, probably due to the outer membrane, cell-penetrating peptide (CPP) DS4.3 was introduced at the N-terminus of PA90 to aid access to its substrate. This engineered endolysin, DS-PA90, completely killed *A. baumannii* at 0.25 μM, at which concentration PA90 could only eliminate less than one log in CFU/ml. Additionally, DS-PA90 has tolerance to NaCl, where the ~50% of activity could be maintained in the presence of 150 mM NaCl, and stable activity was also observed with changes in pH or temperature. Even MDR *A. baumannii* strains were highly susceptible to DS-PA90 treatment: five out of nine strains were entirely killed and four strains were reduced by 3–4 log in CFU/ml. Consequently, DS-PA90 could protect waxworm from *A. baumannii*-induced death by ~70% for ATCC 17978 or ~44% for MDR strain 1656-2 infection. Collectively, our data suggest that CPP-fused endolysin can be an effective antibacterial agent against Gram-negative pathogens regardless of antibiotics resistance mechanisms.

Keywords: bacteriophage, endolysin, cell-penetrating peptide, *Acinetobacter baumannii*, multiple drug-resistant

*For correspondence. E-mail: songm@hufs.ac.kr
[§]Supplemental material for this article may be found at https://doi.org/10.1007/s12275-022-2107-y.

Introduction

Bacterial infections can be efficiently cured by treatment with antibiotics, but a shortage of available antibiotics is closely related with infection-induced death, which is a result of the emergence of multiple drug-resistant (MDR) bacteria. As a representative MDR bacteria, *A. baumannii* is resistant to most clinical antibiotics by using various mechanisms such as efflux pumps, β-lactamases, aminoglycoside-modifying enzymes, permeability defects, and the alteration of target sites (Lin and Lan, 2014; Lee *et al.*, 2017). In particular, the high genetic plasticity of *A. baumannii* results in a reservoir of resistance genes by horizontal transfer, particularly using mobile genetic elements including integrons (Lin and Lan, 2014; Pagano *et al.*, 2016). Therefore, it is urgent to develop alternative antimicrobials for the treatment of *A. baumannii* infection, with possibly low frequency of resistance.

Attention has been paid to bacteriophage as an alternative agent(s) for the control of bacterial infection. As viruses of bacteria, phages can infect specific hosts depending on receptor binding proteins and kill the host bacteria when reproduction is completed. Even biofilms and extracellular matrix can be disrupted by phages (Azeredo and Sutherland, 2008; Walsh *et al.*, 2021). Additionally, the genetic engineering is relatively less troublesome due to simple genetic composition (Meile *et al.*, 2022). Indeed, there is increasing evidence that shows the potential of phages or engineered phages as a treatment option without or together with antibiotics for bacterial infections including MDR bacteria (Bhargava *et al.*, 2021; Walsh *et al.*, 2021; Blasco *et al.*, 2022; Sisakhtpour *et al.*, 2022; Xuan *et al.*, 2022). Despite the benefits of phages as antimicrobials, drawbacks such as restricted host range and the emergence of phage resistance are also evident (Meile *et al.*, 2022).

Phage endolysins are peptidoglycan hydrolases that mediate the release of phage progeny (Fischetti, 2010). The addition of purified recombinant endolysin causes immediate lysis and death of Gram-positive bacteria *in vitro* (Fenton *et al.*, 2010). In addition, administration of endolysin was shown to be effective in reducing a colonized Gram-positive pathogen in an animal model (Loeffler *et al.*, 2001; Nelson *et al.*, 2001; Cheng *et al.*, 2005). Currently, endolysins targeting Gram-positive pathogens are in the development stage for clinical treatment in humans where natural endolysins were mined and improved by protein engineering with increased antimicrobial activity, followed by additional protein and biochemical engineering. Also, formulations have been designed for improving half-life, bioavailability, and antimicrobial activity (De Maesschalck *et al.*, 2020). However, the activity of endolysin is less effective against Gram-negative bacteria due to the outer membrane

(OM), which limits the accessibility of endolysin to peptidoglycan.

Cell-penetrating peptide (CPP) is a short peptide with the ability of crossing the cell membrane and is widely applied for the intracellular delivery of molecules such as peptides, proteins, nucleic acids, and nanoparticles (Derakhshankhah and Jafari, 2018; Sadeghian *et al.*, 2022). For medical applications, CPP has been used as a delivery tool for cancer therapy including DS4.3 (Jeong *et al.*, 2014), inflammation therapy (Lee *et al.*, 2012), and vaccine development (Sadeghian *et al.*, 2022), and is expanding to other areas. More importantly, CPP has been used against bacteria by binding and disturbing the membrane, which is more negatively charged than mammalian cells (Oikawa *et al.*, 2018; Drexelius *et al.*, 2021). Also, conjugation of CPP to antibacterial agents has been used for the delivery of agents into the cytoplasm of infected cells where the agents kill intracellular pathogens efficiently (Chen *et al.*, 2021; Frimodt-Møller *et al.*, 2022; Rüter, 2022).

Here, we mined a novel endolysin from a newly identified *Pseudomonas* phage in an endeavor to develop an alternative control agent for MDR *A. baumannii* infection. From genome analysis, one gene was predicted to be endolysin and named as PA90, which was then cloned for overexpression. The purified recombinant protein was shown to have moderate antibacterial activity against *A. baumannii*. Subsequently, CPP DS4.3 was introduced at the N-terminus of PA90 to increase the efficiency of endolysin. This engineered endolysin could completely kill not only laboratory strains but also drug-resistant strains of *A. baumannii in vitro* and tolerance to high concentrations of NaCl, which limited the application of endolysins, was improved. Finally, DS-PA90 could protect waxworm from *A. baumannii* infection including MDR strains. Therefore, our study suggests that the introduction of CPP to endolysin can enhance the function against Gram-negative pathogens such as MDR *A. baumannii*.

Materials and Methods

Bacterial strains and growth conditions

Pseudomonas aeruginosa ATCC 13388, *Escherichia coli* ATCC 8739, *Acinetobacter baumannii* ATCC 17978, *Klebsiella pneumoniae* KTCC 2208, *Enterobacter aerogenes* CCARM 16006, *Enterobacter cloacae* CCARM 0252 were purchased from the American Type Culture Collection (ATCC), the Korean Collection for Type Cultures (KCTC), and the Culture Collection of Antimicrobial Resistance Microbes (CCARM). The clinical isolates of *A. baumannii* were obtained from the Kyungpook National University Hospital National Culture Collection for Pathogens (KNUH-NCCP). All bacterial strains were grown in Luria Bertani (LB; MBcell MB-L4488) broth at 37°C with vigorous aeration at 200 rpm.

Bacteriophage PBPA90 genome analysis and bioinformatic analysis of endolysin PA90

Bacteriophage was isolated from Opo Wastewater Facility in Gwangju, Gyeonggi-do, Korea by the soft agar overlay method. In brief, three milliliters of wastewater and 100 ml of cultured *P. aeruginosa* at log phase (OD_{600} = 0.5) were added to an LB soft agar (final 0.7%) and then the mixture was overlayed on an LB agar plate. After overnight incubation at 37°C, a single plaque was selected for the purification of phages by centrifugation using 10% (w/v) polyethylene glycol 8000 (PEG 8000) (Kim *et al.*, 2015). The purified phage was named PBPA90. The genomic DNA of PBPA90 was isolated using a phage DNA isolation kit (Norgen #46800) and whole genome sequences were identified by Illumina Miseq (LAS) using the genomic library prepared by the Truseq® Nano DNA sample preparation kit with 150 bp paired-end DNA reads. SAVAGE was used for genome assembly and annotation (Baaijens *et al.*, 2017), followed by remapping to sequence reads and manual curation. Open reading frames (ORFs) were analyzed using BLAST and the putative endolysin was identified by comparison to the COG, SwissProt, and Pfam database: endolysin PA90 (GenBank accession number: MW815133). The domain architecture of PA90 was predicted by the InterPro tool (Quevillon *et al.*, 2005) and the secondary/tertiary structure was predicted by Phyre server (Kelley and Sternberg, 2009).

Construction of the PA90 or DS-PA90 expression plasmid

The putative endolysin PA90 was amplified by PCR with the primers forward 5′-aaGGATCCATGGGTACTGTACTCAAACGTGGC-3′ and reverse 5′-aaCTCGAGTGCCCGATGTTTCGAAACTTTATCTTC-3′. The 793 bp PCR product was cleaned up with Qiagen clean up kit (#28204) and digested with BamH1 (NEB#R3136S) and Xho1 (NEB#R0146L). The digested DNA fragment was ligated with pET21-a (+), generating pAS-025. The cell-penetrating peptide DS4.3 (RIMRILRILKLAR) was introduced by PCR using pAS025 as a template with forward primer 5′-GCATTCTGAAACTGGCGCGTATGGGTACTGTACTCAAACGTGGC-3′ and reverse primer 5′-GCAGAATACGCATAATGCGACCGCCGCCCTGGAAGTAAA-3′. The PCR product was treated with Dpn1 (NEB #R0176L) for the removal of the template and a DNA band with the expected size was extracted from the agarose gel. The cleaned DNA fragment was circularized by ligation in the presence of polynucleotide kinase (PNK; NEB #M0236L), yielding pAS033. The plasmids were confirmed by sequencing analysis. Each plasmid, pAS025 or pAS033, was introduced into BL21 (DE3) pLysS or SoluBL21™, respectively, for the purification of endolysins.

Purification of PA90 or DS-PA90

BL21 strain carrying pAS025 or pAS033 was grown in 1.5 L of LB broth containing ampicillin (100 mg/ml) at 37°C until the optical density at 600 nm reached 0.6. Protein expression was induced by the addition of 1 mM isopropyl-β-D-thiogalactopyranoside (IPTG) and bacteria were further cultured at 37°C for 4 h. The cells were harvested by centrifugation at 5,000 × *g* for 10 min at 4°C. The bacterial pellet was resuspended in 100 ml of lysis buffer [20 mM Tris-HCl; pH 7.5, 0.5 M NaCl, 10 mM imidazole] and disrupted by sonication on ice. The unbroken cells were separated by centrifugation at 14,000 × *g* for 30 min at 4°C and the supernatant fraction was filtered through a 0.4 μM pore size filter (GVS #FJ25ASCCA004FL01). The collected fraction containing

N-terminal 6× histidine tagged endolysin was applied to 5 ml of HisTrap HP column (Cytiva #17524802) installed in an ÄKTA go fast protein liquid chromatography (FPLC) system (Cytiva) controlled by UNICORN 5.1 software. The bound endolysins were eluted using a buffer [20 mM Tris-HCl; pH 7.5, 0.5M NaCl] with gradient of imidazole concentration from 10 mM to 0.5 M and the eluted fractions containing endolysins were then applied into a 5 ml of HisTrap SP column (Cytiva #17-1152-01). The proteins were bound to the resin in 20 mM Tris-HCl; pH 7.5 and eluted with another buffer [20 mM Tris-HCl; pH 7.5, 1 M NaCl]. Fractions were collected and dialyzed overnight in 20 mM Tris-HCl; pH 7.5 and 150 mM NaCl at 4°C. The protein concentration was measured with a Bradford assay kit (Bio-Rad# 5000006).

Measurement of antibacterial activity of PA90 or DS-PA90 by CFU reduction assay

The lytic spectrum of PA90 was determined using *Pseudomonas aeruginosa*, *Escherichia coli*, *Acinetobacter baumannii*, *Klebsiella pneumoniae*, *Enterobacter aerogenes*, and *Enterobacter cloacae* as host strains. Bacterial cells were grown in LB broth at 37°C and cells were harvested by centrifugation at 15,000 × *g* for 1 min when the growth reached the mid-exponential phase (OD_{600} = 0.8). The cell pellet was washed and resuspended in 20 mM Tris-HCl; pH 7.5 then mixed with 0, 0.2, 2 μM of the purified PA90 in 96-well. After 2 h incubation at 37°C, cells were serially diluted in 1 × PBS and plated on LB agar to determine the surviving number of bacteria. For antibiotic-resistant *A. baumannii* strains including clinical isolates, the bacteria were treated with 0 and 0.25 μM of PA90 or DS-PA90, respectively, for the comparison of enzyme activity.

Determination of optimal salt concentration, pH, and temperature for the activity of DS-PA90

Freshly grown *A. baumannii* ATCC 17978 cells were prepared as mentioned above and treated with 2 μM of PA90 or 0.125 μM of DS-PA90. For the optimal pH test, each endolysin was incubated in 20 mM Tris-HCl solution adjusted to pH 5.0, 6.5, 7.5, 8.5 and 10.0, respectively, at room temperature for 1 h and then used for a CFU reduction assay. Sodium chloride was added to 20 mM Tris-HCl; pH 7.5 buffer as final 0, 25, 50, 100, and 150 mM for a salt concentration test and the mixture of bacterial cells and each endolysin was incubated at 37°C for 2 h. The thermal stability of endolysins was determined by the pre-incubation of endolysins at 15, 25, 37, 45, and 55°C for 1 h. The bacteria resuspended in 20 mM Tris-HCl; pH 7.5 was then treated with preincubated PA90 or DS-PA90 at 37°C. After 2 h, the diluted samples were plated on LB agar and incubated at 37°C overnight. The next day, the bacterial numbers were counted and the percent of relative reduction was calculated as the percent of bacteria killed under the given condition referring to the assay conditions in 20 mM Tris-HCl; pH 7.5 at 37°C.

Determination of minimum inhibitory concentrations (MICs) of *A. baumannii* clinical isolates

The MIC of antibiotics were determined by broth microdilution method in 96-well plates as described previously (Hong *et al.*, 2022). Each clinical isolate of *A. baumannii* was grown in LB overnight and inoculated into fresh CAA medium (5 g/L casamino acids, 5.2 mM K_2HPO_4, and 1 mM $MgSO_4$). The culture was then grown at 37°C for 3.5 h. The cells were diluted to 1×10^4 CFU/well in CAA medium and incubated with antibiotics (colistin, cefotaxime, ciprofloxacin, meropenem, gentamicin, and tetracycline) at 37°C for 20 h. The MIC values were determined as the lowest concentration for inhibiting bacterial growth completely.

Galleria mellonella infection model for DS-PA90 treatment

Healthy larvae of greater wax moth, *Galleria mellonella*, were obtained from Sworm. Larvae were selected to be in the final instar stage and weigh from 80 to 140 mg. Before bacterial infection, larvae were fastened and kept in the dark at 30°C for 24 h. Overnight culture of *A. baumannii* ATCC 17978 or clinical isolate 1656-2 (Park *et al.*, 2011) strain was inoculated into fresh LB and cultured for 2 h for infection into the larvae. The bacterial cultures were then harvested by centrifugation at 4,500 rpm for 3 min and resuspended in 1 × PBS. Immediately before injection, 10 μM of DS-PA90 was mixed with 2×10^6 CFU of each bacterial suspension and the mixture was injected into the last-left-proleg using a 10R-GT 10 ml syringe (Trajan Scientific and Medical, 002200) (n = 10). Larvae were then incubated at 30°C for 72 h and their survival were monitored by checking the response to touch and melanization of the whole body. As a control, the same amount of 1 × PBS was mixed with bacterial suspension and injected into larvae (mock; n = 10). The experiment was repeated at least three times.

Statistical analysis

Data analysis was carried out using GraphPad Prism software version 9.3.0. A two-tailed Student's t-test was used for the analysis of the differences between the two groups and a log-rank (Mantel-cox) test was used for survival experiments. All data are presented as mean ± SD, and differences were considered significant at $P < 0.05$.

Results

Identification of new *Pseudomonas* phage PBPA and its endolysin PA90

A library of bacteriophages from a sewage water treatment facility was screened and a phage from the library formed a single plaque on a soft agar plate containing *Pseudomonas aeruginosa* ATCC 13388, which was named PBPA. A circular genome of PBPA was 304,052 bp in length, which has 98.53% identity compared to *Pseudomonas* phage PA1C with 99% coverage by BLAST analysis with whole genome sequencing results. There were 241 predicted ORF by NCBI ORF finder and analyzed by BLAST (Supplementary data Fig. S1) and one of them was a putative endolysin, PA90. BlastP analysis showed that the amino acid sequence of PA90 is 99.23% identical to the putative endolysin of *Pseudomonas* phage PA1C (GenBank accession number: QBX32324.1) and 57.2% identical to the putative endolysin of *Pseudomonas* phage KTN4 (GenBank accession number: ANM44938.1) (Fig. 1A). Func-

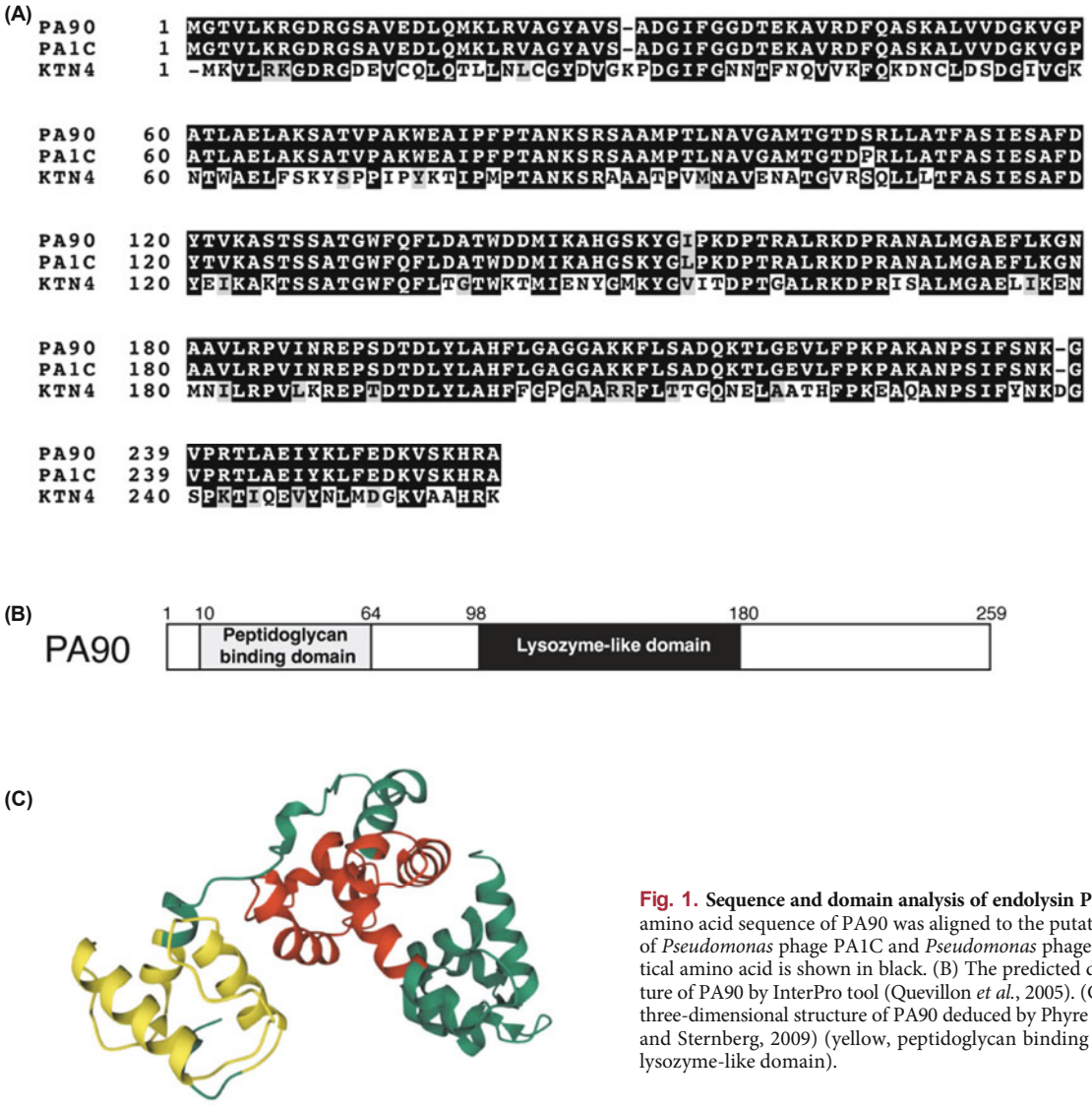

Fig. 1. Sequence and domain analysis of endolysin PA90. (A) The amino acid sequence of PA90 was aligned to the putative endolysin of *Pseudomonas* phage PA1C and *Pseudomonas* phage KTN4. Identical amino acid is shown in black. (B) The predicted domain structure of PA90 by InterPro tool (Quevillon *et al.*, 2005). (C) The overall three-dimensional structure of PA90 deduced by Phyre server (Kelley and Sternberg, 2009) (yellow, peptidoglycan binding domain; red, lysozyme-like domain).

tional domain analysis and structural alignment revealed a peptidoglycan-binding domain (aa 10-64) and a lysozyme-like domain (aa 98-180) (Fig. 1B). The predicted tertiary structure was 55.8% similar to the *Pseudomonas* bacteriophage PhikZ lytic transglycosylase (PDB ID: 3BKH) (Fig. 1C). Therefore, a new *Pseudomonas* phage, PBPA, was isolated and a putative endolysin, PA90, was identified.

Endolysin activity of PA90 and engineered PA90 (DS-PA90) against *A. baumannii*

To verify endolysin activity, the recombinant PA90 with 6× His tag at the C-terminus was purified from BL21 (DE3) pLysS strain using FPLC with a HisTrap HP column (Fig. 2A). The antibacterial activity of the purified PA90 was tested against *P. aeruginosa*, *K. pneumoniae*, *A. baumannii*, *E. aerogenes*, *E. cloacae*, and *E. coli* (Fig. 2B). Most bacterial strains were not affected by 0.2 μM PA90, except *E. cloacae*, and *E. coli*, the numbers of which decreased 10- and 7.9-fold, respectively. The number of bacteria further decreased by treatment with 2 μM PA90 for 2 h for all tested strains, where the reduction fold ranged from 2 to 150. Among the tested bacteria, *P. aeruginosa,* the original host for PBPA, and *A. baumannii* were most effectively killed by treatment with PA90, and their numbers were reduced 150- and 60-fold, respectively. However, PA90 could not eliminate either bacteria completely. Therefore, engineering of PA90 was pursued to increase lytic activity, especially against our target bacteria, *A. baumannii*. To this end, the cell-penetrating peptide DS4.3 (RIMRILRILKLAR; Jeong *et al.*, 2014) was introduced at the N-terminus of PA90 to aid the penetration of endolysin into the outer membrane of Gram-negative bacteria (Fig. 2C). The engineered PA90, named DS-PA90, was purified from BL21 (DE3) SoluBL21^{TM} using His tag at the C-terminus by affinity purification (Fig. 2D). Of note, DS4.3 fused PA90 slightly formed aggregates when it was induced by 1 mM IPTG at 37°C for 5 h (Supplementary data Fig. S2). Next, the antibacterial activity of DS-PA90 was determined using *A. baumannii* 17978 grown at exponential phase in comparison with PA90 (Fig. 2E). The number of *A. baumannii* slightly de-

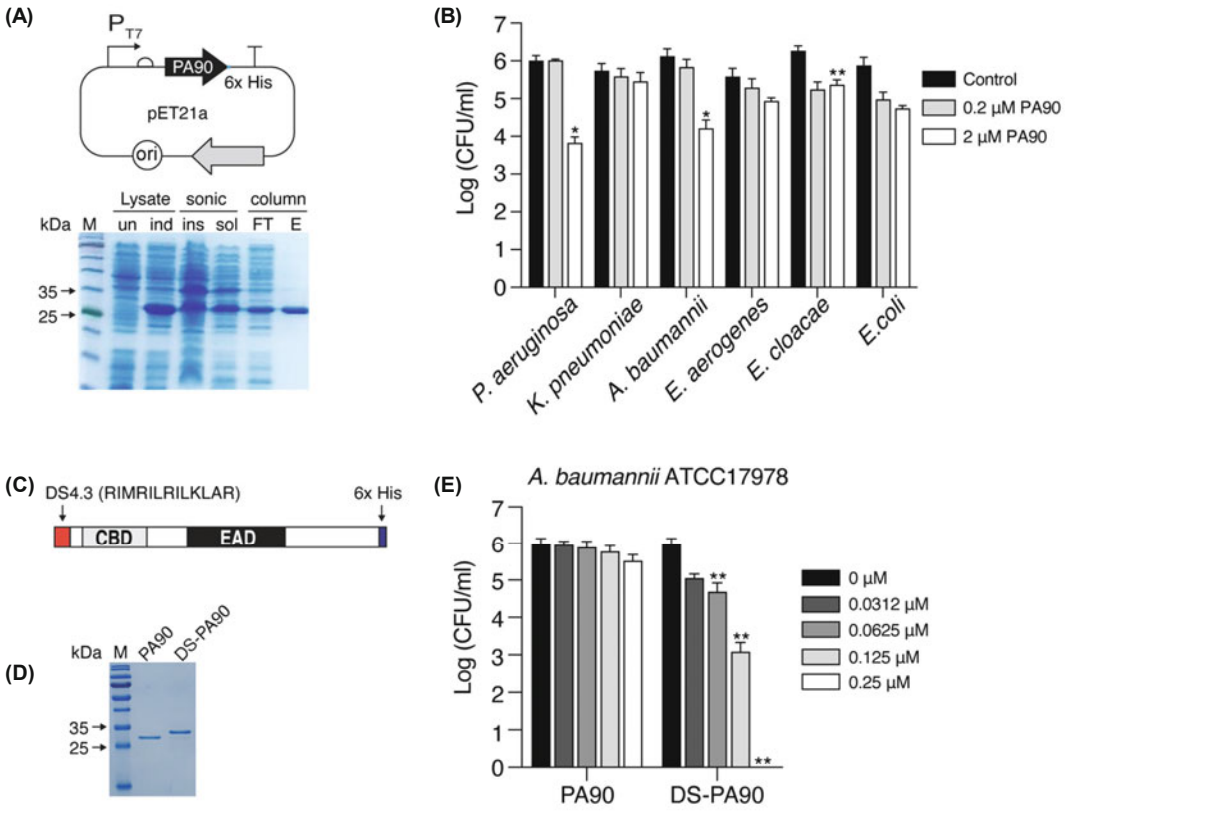

Fig. 2. Antibacterial spectrum of endolysin PA90 and endolysin activity of the engineered DS-PA90 against *A. baumannii* 17978. (A) The gene encoding PA90 was cloned in pET21a (map) and 6× His-tagged PA90 was purified from BL21(DE3) pLysS strain using FPLC and analyzed by 10% SDS-PAGE. The samples were taken during the purification procedure. Total lysate of uninduced (un) and induced (ind) was compared and sonicated lysate was separated into insoluble (ins) and soluble (sol) fractions. The soluble fraction was applied to the column of FPLC and PA90 was detected from flow-through (FT) and eluted (E) fractions. (B) A CFU reduction assay was performed using exponentially grown cells (OD_{600} = 0.8) of *P. aeruginosa*, *K. pneumoniae*, *A. baumannii*, *E. aerogenes*, *E. cloacae*, and *E. coli*. Each strain resuspended in 20 mM Tris-HCl; pH 7.5 was mixed with 0, 0.2, and 2 μM of the purified PA90 and the mixture was incubated at 37°C for 2 h. The surviving numbers of bacterial cells were enumerated by plating on an LB agar plate after serial dilution. Significance is indicated as $^{*}P < 0.04$; $^{**}P = 0.0042$. (C) Domain structure of DS-PA90. DS4.3 (RIMRILRILKLAR) was fused to the N-terminus of PA90. (D) Purified recombinant PA90 and DS-PA90 using FPLC. (E) The lytic activity of DS-PA90 was determined using *A. baumannii* 17978 strain by CFU reduction assay. The bacterial cells were treated with 0, 0.032, 0.0625, 0.125, and 0.25 μM PA90 or DS-PA90, respectively. Significance is shown as $^{**}P \leq 0.0065$. Experiments were repeated at least three times and data are presented as mean ± SD.

creased from 1×10^6 to 3.4×10^5 by 0.25 μM PA90, whereas more bacteria were killed by 0.0312 μM DS-PA90 and half of the bacterial population was removed by 0.125 μM DS-PA90. Finally, bacterial cells were completely eliminated by 0.25 μM DS-PA90. Of note, antibacterial activity of DS-PA90 was also improved against *P. aeruginosa*, *K. pneumoniae*, *E. coli*, *E. aerogenes*, and *E. cloacae* (Supplementary data Fig. S3) but, DS-PA90 was most effective against *A. baumannii*. Therefore, the endolysin activity of PA90 was improved by the addition of DS4.3 peptide at N-terminus, which might help the penetration of the outer membrane of *A. baumannii*.

Effect of salinity, pH and temperature on lytic activity of DS-PA90

Next, the endolysin activity of DS-PA90 was tested under environmental stresses including salinity, pH and temperature. The maximal activity of DS-PA90 was observed when the assay was performed in the reaction buffer either without NaCl or in the presence of 25 mM NaCl, but gradually decreased as the concentration of NaCl was increased. The

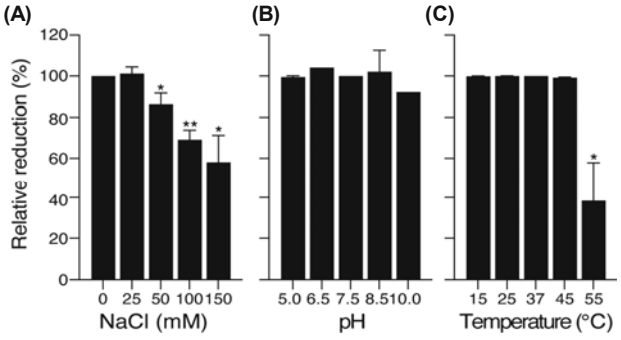

Fig. 3. Lytic activity of DS-PA90 upon changes in NaCl concentration, pH and temperature. A CFU reduction assay was performed with 0.125 μM DS-PA90 using freshly grown *A. baumannii* ATCC 17978 cells in buffer containing different concentrations of NaCl (A). DS-PA90 was pre-incubated in buffer with different pH (B) or at different temperatures (C) for 1 h and then used for the assay. The percent of relative reduction was calculated as the percent of bacteria killed in a given condition, referring to the assay condition in 20 mM Tris-HCl; pH 7.5 at 37°C. Significance is indicated as $^{*}P < 0.049$; $^{**}P < 0.007$. Experiments were repeated at least three times and data are presented as mean ± SD.

Table 1. Minimum inhibitory concentrations (μg/ml) of the clinical isolates of *A.baumannii*

Strains	Colistin	Cefotaxime	Ciprofloxacin	Meropenem	Gentamicin	Tetracycline
1656-2	16	64 ≥	64	64 ≥	64 ≥	64
3097	64	64	63	64	64 ≥	64
365	8	32	1	32	2	4
643	64 ≥	64 ≥	64 ≥	64 ≥	64 ≥	64 ≥
4316	64 ≥	32	64	8	64 ≥	32
2496	64 ≥	32	1	32	8	4
205	8	64	1	4	8	4
216	8	32	4	64	8	1
3680	64	32	4	64	16	2

activity of DS-PA90 decreased approximately 30% by the addition of 100 mM NaCl, and 58% of activity was maintained in the buffer with 150 mM NaCl compared to the buffer without NaCl for CFU reduction assay (Fig. 3A). Thus, the engineered PA90 was shown to be stable under osmotic stress. Of note, the remaining activity of PA90 was only 10% in the buffer containing 150 mM NaCl for CFU reduction assay (Supplementary data Fig. S4). The stability of DS-PA90 was also tested with changes in pH or temperature. The antibacterial activity of DS-PA90 decreased less than 8% after pre-incubation of endolysin in the reaction buffer with different pH ranging from 5 to 10. Also, the thermal stability of DS-PA90 was measured by CFU reduction assay after pre-treatment of endolysin at different temperatures. The lytic activity of DS-PA90 was maintained well after pre-treatment of protein at 15, 25, 37, and 45°C, but the activity decreased up to 60% after pre-treatment at 55°C. Collectively, the stable lytic activity of DS4.3 fused PA90 was observed upon the challenges of pH and temperature stress.

Antibacterial activity of DS-PA90 in waxworm, *Galleria mellonella*

Since the potential of DS-PA90 as an alternative antibiotics was tested using a standard laboratory strain of *A. baumannii* (ATCC 17978), the antibacterial activity was further investigated against clinical isolates of *A. baumannii*. First, a total of nine clinical isolates were screened for susceptibility to antibiotics by the measurement of minimum inhibitory concentrations (MICs) (Table 1). All tested strains were either intermediate or resistant to cefotaxime, meropenem, gentamicin, except strain 365 for gentamicin. Several strains were susceptible to ciprofloxacin and tetracycline. Collectively, each strain was shown to be resistant to at least two antibiotics; thus, all clinical isolates were regarded as multiple drug-resistant strains. Next, the antibacterial activity of DS-PA90 was tested against such antibiotic-resistant clinical isolates (Fig. 4A). Strains 365, 1656-2, 216, and 643 were completely killed, and ~4 log number of four strains (3097, 4316, 2496, and 205) were eliminated by DS-PA90 treatment. Therefore, the lytic activity of DS4.3 fused PA90 was also effective in multiple drug-resistant strains of *A. baumannii in vitro*. Finally, the efficacy of DS-PA90 was determined using waxworm, *G. mellonella*, as an *in vivo* model system with *A. baumannii* ATCC 17978 or clinical isolate 1656-2. Each strain was diluted in PBS containing 2×10^6 CFU and DS-PA90 was added to the cell suspension immediately before injection, which did not lead to bacterial killing (data not shown). Larval death was observed in the group infected with either strain and treatment with DS-PA90 increased the survival of infected larvae up to ~70% with ATCC 17978 or ~44% with clinical isolate 1656-2 strain (Fig. 4B and C). Therefore, it was clearly shown that DS-PA90 can kill multidrug-resistant strains of *A. baumannii* and effectively control bacterial infection in waxworm.

Discussion

Endolysin is a promising agent to replace or support antibiotics with high specificity against bacteria and low probability of resistance (Dams and Briers, 2019). However, the enzymatic activity of endolysin is restricted to its substrate, peptidoglycan, resulting in the limited application of endo-

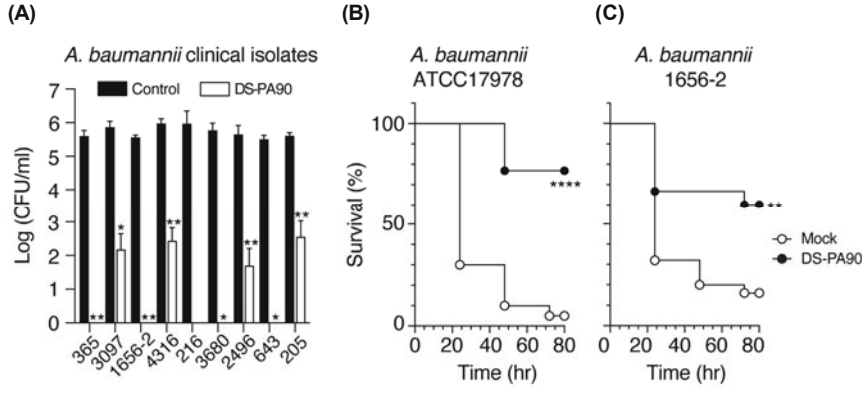

Fig. 4. Antibacterial activity of DS-PA90 against MDR *A. baumannii in vitro* and in *Galleria mellonella*. (A) The lytic activity of DS-PA90 was determined using clinical isolates of *A. baumannii* strains by CFU reduction assay. Significance is indicated as $^*P < 0.031$; $^{**}P < 0.008$. Data are presented as mean ± SD (n = 3). The larvae of *Galleria mellonella* were infected by 2×10^6 CFU *A. baumannii* ATCC 17978 (B) or clinical isolate 1656-2 (C) strain. For endolysin treatment, 10 μM of DS-PA90 was mixed with bacterial suspension immediately before injection. As a control, the same amount of 1× PBS was used (mock). The survival of larvae was monitored while the larvae were kept at 30°C for 72 h (n = 10 per group). The experiment was repeated three times. Significance is shown as $^{****}P < 0.0001$; $^{**}P = 0.0047$.

lysin for Gram-negative pathogens containing an outer membrane. Therefore, engineering is required to develop endolysin to eliminate Gram-negative bacteria including *A. baumannii*.

Here, we identified a new *Pseudomonas* bacteriophage, PBPA-90, from the environment and mined a putative endolysin, PA90, by bioinformatic analysis. Since the bactericidal activity of the purified PA90 was shown to be weak, the endolysin was engineered where a cell-penetrating peptide (CPP) DS4.3 was introduced at the N-terminus of PA90. The resulting endolysin, DS-PA90, could completely eliminate *A. baumannii* cells *in vitro*. Although the role of DS4.3 is known for the eukaryotic cell membrane, this peptide can help the penetration of the outer membrane of bacteria, which has positive chwarge and was suggested for other CPPs against bacteria (Oikawa *et al.*, 2018; John *et al.*, 2019). Also, its increased stability might be related to the improved activity of DS4.3 fused endolysin. In particular, the activity of PA90 was hindered by a high concentration of NaCl, but fusion of DS4.3 buffered the impact of the increased concentration of NaCl on the enzymatic activity of PA90. However, the role of DS4.3 should be addressed in future studies to elucidate the feasibility of this CPP for the development of engineered endolysins against Gram-negative pathogens. It was shown that certain CPPs can efficiently disrupt bacterial membranes due to their chemical characteristics such as net positive charge, which aid the binding of peptides to negatively charged bacterial membranes (Derakhshankhah and Jafari, 2018; Oikawa *et al.*, 2018). By fusing CPP to endolysin, this enzyme can be a more powerful antibacterial agent.

Most importantly, the antibacterial activity of DS-PA90 was extremely effective against clinical isolates of *A. baumannii* with multiple drug resistance such as β-lactam antibiotics, aminoglycoside and tetracycline. Furthermore, the endolysin activity of DS-PA90 could rescue waxworm from *A. baumannii* infection-induced death. But the *in vivo* activity of DS-PA90 should be tested in an animal model to prove the potential of this engineered endolysin as alternative agent for *A. baumannii* infection in a future study. Also, the synergistic effect of DS-PA90 can be determined in combination with a variety of antibiotics, which is also pursued for other endolysins (De Maesschalck *et al.*, 2020).

There are many excellent features of endolysin, which include a broad spectrum of hosts, high antibacterial activity, and low rates of resistance (Lai *et al.*, 2020). But when it comes to practical application, endolysins are not as effective as in the *in vitro* condition. It was observed that the majority of endolysins were deposited in the kidneys like other peptide- or protein-based drugs (Seijsing *et al.*, 2018; Sobieraj *et al.*, 2020). A short half-life in serum was reported, and low accessibility to intracellular pathogens was also noticed (Seijsing *et al.*, 2018; Schmelcher and Loessner, 2021; Sobieraj *et al.*, 2020). Protein engineering can help overcome such limitations, including the fusion of albumin binding domain (ABD) or domain shuffling of multiple endolysins or addition of CPP (Sobieraj *et al.*, 2020).

In our study, we demonstrated that the addition of CPP to endolysin enhanced antibacterial activity against MDR *A. baumannii* and stability of protein *in vitro*. Therefore, our findings pave the way for new designed drugs to treat infection by drug-resistant pathogens.

Acknowledgements

This work was supported by the National Research Foundation of Korea grant funded by the Korean government (2021R1F1A1060072 and 2019M3E5D5066666), and by the Hankuk University of Foreign Studies Research Fund (of 2022).

Conflict of Interest

The authors have no conflict of interest to report.

References

Azeredo, J. and Sutherland, I.W. 2008. The use of phages for the removal of infectious biofilms. *Curr. Pharm. Biotechnol.* **9**, 261–266.

Baaijens, J.A., Aabidine, A.Z.E., Rivals, E., and Schönhuth, A. 2017. *De novo* assembly of viral quasispecies using overlap graphs. *Genome Res.* **27**, 835–848.

Bhargava, K., Nath, G., Bhargava, A., Aseri, G.K., and Jain, N. 2021. Phage therapeutics: from promises to practices and prospectives. *Appl. Microbiol. Biotechnol.* **105**, 9047–9067.

Blasco, L., Bleriot, I., González de Aledo, M., Fernández-García, L., Pacios, O., Oliveira, H., López, M., Ortiz-Cartagena, C., Fernández-Cuenca, F., Pascual, Á., *et al.* 2022. Development of an anti-*Acinetobacter baumannii* biofilm phage cocktail: genomic adaptation to the host. *Antimicrob. Agents Chemother.* **66**, e0192321.

Chen, H., Battalapalli, D., Draz, M.S., Zhang, P., and Ruan, Z. 2021. The application of cell-penetrating-peptides in antibacterial agents. *Curr. Med. Chem.* **28**, 5896–5925.

Cheng, Q., Nelson, D., Zhu, S., and Fischetti, V.A. 2005. Removal of group B streptococci colonizing the vagina and oropharynx of mice with a bacteriophage lytic enzyme. *Antimicrob. Agents Chemother.* **49**, 111–117.

Dams, D. and Briers, Y. 2019. Enzybiotics: Enzyme-Based Antibacterials as Therapeutics. *In* Labrou, N. (eds), Therapeutic Enzymes: Function and Clinical Implications. Advances in Experimental Medicine and Biology, vol. 1148, pp. 233–253. Springer, Singapore.

De Maesschalck, V., Gutiérrez, D., Paeshuyse, J., Lavigne, R., and Briers, Y. 2020. Advanced engineering of third-generation lysins and formulation strategies for clinical applications. *Crit. Rev. Microbiol.* **46**, 548–564.

Derakhshankhah, H. and Jafari, S. 2018. Cell penetrating peptides: a concise review with emphasis on biomedical applications. *Biomed. Pharmacother.* **108**, 1090–1096.

Drexelius, M., Reinhardt, A., Grabeck, J., Cronenberg, T., Nitsche, F., Huesgen, P.F., Maier, B., and Neundorf, I. 2021. Multistep optimization of a cell-penetrating peptide towards its antimicrobial activity. *Biochem. J.* **478**, 63–78.

Fenton, M., Ross, P., McAuliffe, O., O'Mahony, J., and Coffey, A. 2010. Recombinant bacteriophage lysins as antibacterials. *Bioeng. Bugs* **1**, 9–16.

Fischetti, V.A. 2010. Bacteriophage endolysins: a novel anti-infective to control Gram-positive pathogens. *Int. J. Med. Microbiol.* **300**, 357–362.

Frimodt-Møller, J., Campion, C., Nielsen, P.E., and Løbner-Olesen, A. 2022. Translocation of non-lytic antimicrobial peptides and bacteria penetrating peptides across the inner membrane of the bacterial envelope. *Curr. Genet.* **68**, 83–90.

Hong, H.W., Kim, Y.D., Jang, J., Kim, M.S., Song, M., and Myung, H. 2022. Combination effect of engineered endolysin EC340 with antibiotics. *Front. Microbiol.* **13**, 821936.

Jeong, J.H., Kim, K., Lim, D., Jeong, K., Hong, Y., Nguyen, V.H.,

Kim, T.H., Ryu, S., Lim, J.A., Kim, J.I., *et al.* 2014. Anti-tumoral effect of the mitochondrial target domain of Noxa delivered by an engineered *Salmonella* Typhimurium. *PLoS ONE* **9**, e80050.

John, C.M., Li, M., Feng, D., and Jarvis, G.A. 2019. Cationic cell-penetrating peptide is bactericidal against *Neisseria gonorrhoeae*. *J. Antimicrob. Chemother.* **74**, 3245–3251.

Kelley, L.A. and Sternberg, M.J.E. 2009. Protein structure prediction on the Web: a case study using the Phyre server. *Nat. Protoc.* **4**, 363–371.

Kim, M.S., Kim, Y.D., Hong, S.S., Park, K., Ko, K.S., and Myung, H. 2015. Phage-encoded colanic acid-degrading enzyme permits lytic phage infection of a capsule-forming resistant mutant *Escherichia coli* strain. *Appl. Environ. Microbiol.* **81**, 900–909.

Lai, W.C.B., Chen, X., Ho, M.K.Y., Xia, J., and Leung, S.S.Y. 2020. Bacteriophage-derived endolysins to target Gram-negative bacteria. *Int. J. Pharm.* **589**, 119833.

Lee, S.H., Kim, D.W., Kim, H.R., Woo, S.J., Kim, S.M., Jo, H.S., Jeon, S.G., Cho, S.W., Park, J.H., Won, M.H., *et al.* 2012. Anti-inflammatory effects of Tat-Annexin protein on ovalbumin-induced airway inflammation in a mouse model of asthma. *Biochem. Biophys. Res. Commun.* **417**, 1024–1029.

Lee, C.R., Lee, J.H., Park, M., Park, K.S., Bae, I.K., Kim, Y.B., Cha, C.J., Jeong, B.C., and Lee, S.H. 2017. Biology of *Acinetobacter baumannii*: pathogenesis, antibiotic resistance mechanisms, and prospective treatment options. *Front. Cell. Infect. Microbiol.* **7**, 55.

Lin, M.F. and Lan, C.Y. 2014. Antimicrobial resistance in *Acinetobacter baumannii*: from bench to bedside. *World J. Clin. Cases* **2**, 787–814.

Loeffler, J.M., Nelson, D., and Fischetti, V.A. 2001. Rapid killing of *Streptococcus pneumoniae* with a bacteriophage cell wall hydrolase. *Science* **294**, 2170–2172.

Meile, S., Du, J., Dunne, M., Kilcher, S., and Loessner, M.J. 2022. Engineering therapeutic phages for enhanced antibacterial efficacy. *Curr. Opin. Virol.* **52**, 182–191.

Nelson, D., Loomis, L., and Fischetti, V.A. 2001. Prevention and elimination of upper respiratory colonization of mice by group A streptococci by using a bacteriophage lytic enzyme. *Proc. Natl. Acad. Sci. USA* **98**, 4107–4112.

Oikawa, K., Islam, M.M., Horii, Y., Yoshizumi, T., and Numata, K. 2018. Screening of a cell-penetrating peptide library in *Escherichia coli*: relationship between cell penetration efficiency and cytotoxicity. *ACS Omega* **3**, 16489–16499.

Pagano, M., Martins, A.F., and Barth, A.L. 2016. Mobile genetic elements related to carbapenem resistance in *Acinetobacter baumannii*. *Braz. J. Microbiol.* **47**, 785–792.

Park, J.Y., Kim, S., Kim, S.M., Cha, S.H., Lim, S.K., and Kim, J. 2011. Complete genome sequence of multidrug-resistant *Acinetobacter baumannii* strain 1656-2, which forms sturdy biofilm. *J. Bacteriol.* **193**, 6393–6394.

Quevillon, E., Silventoinen, V., Pillai, S., Harte, N., Mulder, N., Apweiler, R., and Lopez, R. 2005. InterProScan: protein domains identifier. *Nucleic Acids Res.* **33**, W116–W120.

Rüter, C. 2022. Delivery of antibiotics by cell-penetrating peptides to kill intracellular pathogens. *Methods Mol. Biol.* **2383**, 335–345.

Sadeghian, I., Heidari, R., Sadeghian, S., Raee, M.J., and Negahdaripour, M. 2022. Potential of cell-penetrating peptides (CPPs) in delivery of antiviral therapeutics and vaccines. *Eur. J. Pharm. Sci.* **169**, 106094.

Schmelcher, M. and Loessner, M.J. 2021. Bacteriophage endolysins - extending their application to tissues and the bloodstream. *Curr. Opin. Biotechnol.* **68**, 51–59.

Seijsing, J., Sobieraj, A.M., Keller, N., Shen, Y., Zinkernagel, A.S., Loessner, M.J., and Schmelcher, M. 2018. Improved biodistribution and extended serum half-life of a bacteriophage endolysin by albumin binding domain fusion. *Front. Microbiol.* **9**, 2927.

Sisakhtpour, B., Mirzaei, A., Karbasizadeh, V., Hosseini, N., Shabani, M., and Moghim, S. 2022. The characteristic and potential therapeutic effect of isolated multidrug-resistant *Acinetobacter baumannii* lytic phage. *Ann. Clin. Microbiol. Antimicrob.* **21**, 1.

Sobieraj, A.M., Huemer, M., Zinsli, L.V., Meile, S., Keller, A.P., Röhrig, C., Eichenseher, F., Shen, Y., Zinkernagel, A.S., Loessner, M.J., *et al.* 2020. Engineering of long-circulating peptidoglycan hydrolases enables efficient treatment of systemic *Staphylococcus aureus* infection. *mBio* **11**, e01781-20.

Walsh, L., Johnson, C.N., Hill, C., and Ross, R.P. 2021. Efficacy of phage- and bacteriocin-based therapies in combatting nosocomial MRSA infections. *Front. Mol. Biosci.* **8**, 654038.

Xuan, G., Lin, H., and Wang, J. 2022. Expression of a phage-encoded Gp21 protein protects *Pseudomonas aeruginosa* against phage infection. *J. Virol.* **96**, e0176921.